Published for SISSA by Springer

Received: *September 19, 2024*
Accepted: *January 4, 2025*
Published: *January 31, 2025*

An exceptional cluster algebra for Higgs plus jet production

Rigers Aliaj [a,b] **and Georgios Papathanasiou** [b,c]

[a] *II. Institut für Theoretische Physik, Universität Hamburg, Luruper Chaussee 149, 22607 Hamburg, Germany*
[b] *Deutsches Elektronen-Synchrotron DESY, Notkestr. 85, 22607 Hamburg, Germany*
[c] *Department of Mathematics, University of London, Northampton Square, EC1V 0HB, London, U.K.*

E-mail: rigers.aliaj@desy.de, georgios.papathanasiou@desy.de

Abstract: A recent evaluation of three-loop nonplanar Feynman integrals contributing to Higgs plus jet production has established their dependence on two novel symbol letters. We show that the resulting alphabet is described by a G_2 cluster algebra, enlarging the C_2 cluster algebra found to cover all previously known integrals relevant for this process. The cluster algebra connection we find reveals new adjacency relations, which significantly reduce the function space dimension of the non-planar triple ladder integral. These adjacencies may be understood in part by embedding G_2 inside higher-rank cluster algebras.

Keywords: Higher-Order Perturbative Calculations, Scattering Amplitudes, Extended Supersymmetry, Higgs Production

ArXiv ePrint: 2408.14544

https://doi.org/10.1007/JHEP01(2025)197

Contents

1 Introduction

Following the discovery of the Higgs boson, a new era of precision measurements has begun at the Large Hadron Collider and its planned High-Luminosity upgrade. Interpreting these measured observables, determining the parameters of the Standard Model as well as telling apart the subtle signature of new physics from them, requires their theoretical description to reach a commensurate level of accuracy. One of the key challenges to this end, remains the computation of scattering amplitudes and their building blocks, Feynman integrals, at higher orders in perturbative quantum field theory [1].

On the analytic front, that often provides a faster and stabler evaluation than the numeric one, the method of choice for computing the master integrals (namely the solutions of the linear integration-by-parts identities [2] among all Feynman integrals contributing to a given process) are differential equations [3–5] in canonical form [6]. Working in dimensional regularisation, where the dimension of loop momenta is $D = 4 - 2\epsilon$, and focusing on bases of integrals $\mathbf{f}$ which evaluate to the often sufficient class of *multiple polylogarithms* [7–9], these canonical differential equations take the form

$$d\mathbf{f}(\vec{z};\epsilon) = \epsilon \left[\sum_i \mathbf{A}_i \, d\log\alpha_i(\vec{z})\right] \mathbf{f}(\vec{z};\epsilon). \tag{1.1}$$

Here, $\vec{z}$ collectively denotes the kinematic variables the integrals depend on, such as external momenta and internal masses, and $d = \sum_j \mathrm{d}z_j \partial_j$ is the total differential. Finally, each α_i is an algebraic function of the $\vec{z}$ components known as a *letter* (of the symbol [10]), with the entire set $\mathcal{A} \equiv \{\alpha_i\}$ similarly denoted as the (symbol) *alphabet*, and $\mathbf{A}_i$ are constant matrices.

JHEP01(2025)197

Despite the great success of the method, for a state-of-the-art application see e.g. [11], this too becomes increasingly unwieldy as the perturbative order and number of kinematic variables grow to meet experimental demands. Serious bottlenecks include analytically solving the integration-by-parts identities in terms of an initial basis, as well as determining the basis transformation that brings it to the form (1.1). However prior knowledge of the alphabet can be extremely helpful with these calculations, as it converts them from symbolic to much simpler, numeric ones [12]. This fact renders the prediction of the alphabet by independent means an attractive endeavour.

In this respect, mathematical objects known as *cluster algebras* [13] appear quite promising. Cluster algebras have been first observed to describe the alphabet of six- and seven-particle amplitudes in planar $\mathcal{N} = 4$ super Yang-Mills theory (SYM) [14], providing crucial information for computing these amplitudes to unprecedented loop orders by bootstrap methods [15–29];[1] and closely related generalisations are also seen to describe higher-point amplitudes of the same theory [35–40]. Most importantly, in [41] it was discovered that cluster-algebraic structures are not confined to idealised models: in particular, it was demonstrated that cluster algebras also underlie the analytic structure of a host of dimensionally regulated Feynman integrals as well as processes in quantum chromodynamics (QCD). Since then, their presence has been confirmed in more examples of integrals [42–50] and imprints of their relevance have also been observed in finite remainders of five-particle QCD amplitudes [51–54]. A review of these developments may be found in Chapter 5 [55] of the SAGEX review on scattering amplitudes [56].

While we will define cluster algebras in more detail in the next section, we can convey their essence with examples of finite rank-two cluster algebras, which will play a central role in what follows: these consist of *cluster variables* a_m for m integer, grouped into unordered sets or *clusters* $\{a_m, a_{m+1}\}$, which may be obtained as rational functions of the variables of the initial cluster, $\{a_1, a_2\}$, by virtue of the *mutation* operation,

$$a_{m+1} = \begin{cases} \frac{1+a_m}{a_{m-1}} & \text{if } m \text{ is odd}\,, \\ \frac{1+a_m^L}{a_{m-1}} & \text{if } m \text{ is even}\,, \end{cases} \tag{1.2}$$

where L is a positive integer with $L \leq 3$. The three inequivalent cases $L = 1, 2, 3$ correspond to the A_2, C_2 and G_2 cluster algebras respectively, echoing the Cartan classification of semi-simple Lie groups of the same rank. For these cases, it's easy to show that $a_{i+4+2^{L-1}} = a_i$, in other words there exist a finite number of nontrivial clusters and cluster variables. For example, in the C_2 case the latter are,

$$\Phi_{C_2} = \{a_1, \ldots, a_6\} = \left\{a_1, a_2, \frac{1+a_2^2}{a_1}, \frac{1+a_1+a_2^2}{a_1 a_2}, \frac{1+2a_1+a_1^2+a_2^2}{a_1 a_2^2}, \frac{1+a_1}{a_2}\right\}. \tag{1.3}$$

[1] Before that, cluster algebras also appeared at the level of the amplitude integrand in this theory [30], as well as enjoyed remarkable connections to other theoretical physics topics, for example thermodynamic Bethe ansätze [31], moduli spaces [32] and electric/magnetic duality [33] of supersymmetric gauge theories, or mirror symmetry [34].

JHEP01(2025)197

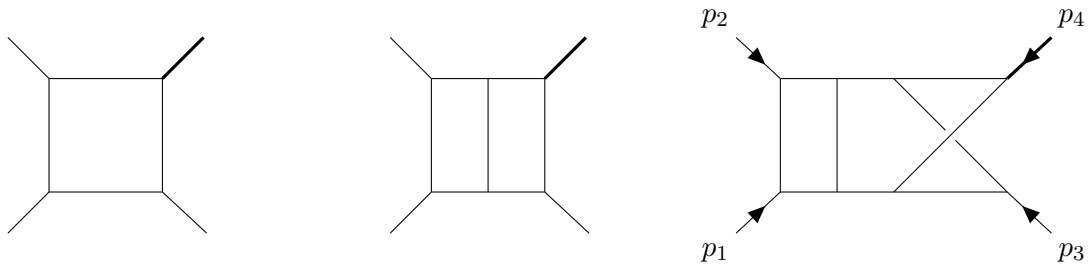

Figure 1. Examples of known integrals with one off-shell leg, $p_4^2 \neq 0$, at (a) one (b) two and (c) three loops. They are described by the A_2, C_2 and G_2 cluster algebras, respectively, with the latter case proven in this work.

The above C_2 cluster algebra was found to describe one of the most prominent classes of Feynman integrals studied in [41], which enter the calculation of amplitudes for Higgs boson plus jet production from proton-proton collisions [57–59] in the heavy-top limit of QCD [60–62]: these were all the known four-point integrals with one off-shell (or equivalently massive) leg, including the complete set of two-loop master integrals [63, 64] as well as L-loop ladders [65, 66]; see figure 1(b) for a representative example. More precisely, all these integrals where shown to obey differential equations of the form (1.1), where the letters α_i coincide (in certain kinematic parametrisation) with the C_2 cluster variables a_i of eq. (1.3)! More three-loop planar integral families confirming the same cluster algebraic structure were also later computed in [67, 68].

Despite this encouraging evidence, a more recent calculation [69], see also [70], has established that the C_2 alphabet (1.3) is in fact too small to describe all integrals with the same kinematics at three loops: in particular, it was found that the three-loop nonplanar ladder integral family depicted in figure 1(c) additionally depends on two novel letters. Does this result cast doubt on the applicability of cluster algebras for Feynman integrals? The main contribution of this work is to demonstrate that *the resulting alphabet in fact corresponds to a G_2 cluster algebra.* We find it remarkable that the alphabets of type A_2, C_2, G_2 become relevant at one, two and three loops, respectively.[2] In other words, the parameter L in eq. (1.2) really seems to be the loop order!

In addition, we study *adjacency restrictions* of the form,

$$\mathbf{A}_i \cdot \mathbf{A}_j = 0, \tag{1.4}$$

for some i, j, of the constant matrices appearing in the differential equations (1.1), for the G_2-alphabet integral family of figure 1(c). In the realm of planar $\mathcal{N} = 4$ SYM theory, adjacency relations appear to encode how the cluster variables arrange themselves into the clusters [71, 72]. They can be in essence physically interpreted as a generalisation [26] of the Steinmann relations [73–75] governing the discontinuities of Feynman integrals and scattering amplitudes, and most importantly, they greatly facilitate bootstrapping the latter by drastically reducing the size of the function space containing them.

[2]Note that the space of polylogarithmic functions with an A_2 alphabet is contained in the space of functions with a C_2 alphabet, and the latter is in turn contained in the space of functions with a G_2 alphabet.

JHEP01(2025)197

For the nonplanar triple ladder integral of figure 1(c), we find 20 inequivalent adjacency relations of the form (1.4) after transforming the original alphabet of ref. [69] to the G_2 cluster variables obtained from eq. (1.2), whereas before the transformation a subset of 16 of these relations were visible. In other words, the cluster algebra connection we find exposes new adjacency relations, and we showcase how these restrict the allowed function space. While these relations are not in one-to-one correspondence with how the G_2 cluster variables are distributed among clusters, we will also show that many of them can be understood by embedding G_2 inside the larger B_3 or D_4 cluster algebras.

The rest of this paper is organised as follows. In section 2 we briefly introduce cluster algebras and their finite type classification, before turning our attention to the rank-two cases, which will be at the heart of this work. We also review how these can be embedded into larger cluster algebras with the process of folding, and define the notion of an embedded neighbour set, which will play an important role when analysing adjacency restrictions.

Then, in section 3 we move on to discuss the alphabet containing all currently computed four-point one-mass integrals through three loops, and, after reviewing certain general procedures for proving the equivalence of alphabets, we apply them to demonstrate that the alphabet in question is described by a G_2 cluster algebra. Section 4 is dedicated to the study of adjacency relations for the single topology with novel letters, the nonplanar triple ladder. We present the adjacency restrictions we observe for the integral in question, we explain them to a great extent with the help of embeddings to larger cluster algebras, and we demonstrate that they indeed lead to a significant reduction in the size of the relevant polylogarithmic function space. Finally, section 5 we present our conclusions and discuss open questions for the future.

2 Basics of cluster algebras

2.1 Definitions and finite type classification

Here we give a brief introduction on the basics of cluster algebras. This relatively new branch of contemporary mathematics, was originally motivated by the study of representation theory and the study of quantum groups [13, 76–78]. However, it appeared to be very useful in many other directions both in terms of mathematics and physics [33, 79–81]. For more details on its mathematical foundations one can follow [82, 83].

For any positive n, a cluster algebra $\mathcal{A}$ of rank n is a commutative ring with unit and no zero divisors. The structure includes a distinguished set of generators $\mathbf{a} \coloneqq \{a_1, a_2, \ldots, a_n\}$, called *cluster variables*, which group into overlapping subsets called *clusters*. The cardinality of each cluster is equal to the *rank* of the cluster algebra. The clusters and the cluster variables are built constructively. One starts from an initial cluster and builds the rest through an operation called *mutation*. The mutation rule is provided by a skew-symmetrisable integer valued $n \times n$ matrix B called the *exchange matrix* with components b_{ij}. Any pair of data $(\mathbf{a}, B)$ is called a *seed*. Mutation leads to new cluster variables and new exchange matrices. Mutation can be performed on any cluster variable and transforms the whole seed. More

JHEP01(2025)197

precisely, mutating $(\mathbf{a}, B)$ on the k-th variable $(1 \leq k \leq n)$ we obtain a new seed $(\mathbf{a}', B')$ with

$$b'_{ij} = \begin{cases} -b_{ij} & \text{for } i = k \text{ or } j = k, \\ b_{ij} + [-b_{ik}]_+ b_{kj} + b_{ik}[b_{kj}]_+ & \text{otherwise,} \end{cases} \tag{2.1}$$

where we denoted $[b_{ij}]_+ = \max(0, b_{ij})$. Moreover, the cluster variables mutate according to

$$a'_i = \begin{cases} a_k^{-1} \left(\prod_{i=1}^n a_i^{[b_{ik}]_+} + \prod_{i=1}^n a_i^{[-b_{ik}]_+} \right) & \text{if } i = k \\ a_i & \text{if } i \neq k \end{cases} \tag{2.2}$$

Consecutive mutations, in principle, produce new variables on each iteration. Note that in any case the number of cluster variables remains the same. When this procedure ends, namely when the cluster variables constitute a finite set, the cluster algebra is said to be of *finite type*. On the contrary, cluster algebras with infinite distinct cluster variables are said to be of *infinite type*.

In this work we will be interested in finite cluster algebras, whose classification is identical to that of semisimple Lie algebras. To this end, one associates a symmetrisable generalised Cartan matrix $A(B)$ to the skew-symmetrisable exchange matrix B of the cluster algebra in the following way

$$a_{ij} = \begin{cases} 2, & \text{if } i = j \\ -|b_{ij}|, & \text{if } i \neq j. \end{cases} \tag{2.3}$$

It has been proven in [13, 76], that cluster algebras are finite if and only if they contain an exchange matrix B such that $A(B)$ is a Cartan matrix of finite type. Therefore, the classification of finite cluster algebras amounts to the classification of finite Cartan matrices into types $A_n, B_n, C_n, D_n, E_6, E_7, F_4, G_2$.

Before moving on to our main example of rank-two finite cluster algebras, let us define two more concepts we will make use of in what follows. The content of a cluster algebra can be visualised in its *exchange graph*, where each cluster is represented as a vertex, and each mutation from a cluster to another as an edge between them. As an explicit example, the exchange graph of the G_2 cluster algebra may be found in figure 2 below. Finally, the *neighbour set* of a cluster variable is the set of all cluster variables appearing with the latter in some cluster.

2.2 The rank-two cluster algebras A_2, C_2, G_2

As stated in the introduction, our main focus will be on the rank two cluster algebras of types A_2, C_2, G_2. These can be obtained by an initial seed with cluster variables $\{a_1, a_2\}$ and exchange matrices given by

$$B = \begin{pmatrix} 0 & 1 \\ -L & 0 \end{pmatrix}, \tag{2.4}$$

where $L = 1, 2, 3$ corresponds to the A_2, C_2, G_2 case, respectively. Indeed, by computing the generalised Cartan matrix of eq. (2.3),

$$A(B) = \begin{pmatrix} 2 & -1 \\ -L & 2 \end{pmatrix}, \tag{2.5}$$

JHEP01(2025)197

we can recognise that it corresponds to the Cartan matrix of the aforementioned rank-two Lie algebras.

Applying the mutation rule of eq. (2.1) to the exchange matrix (2.4), it is easy to check that it only switches sign. Since the corresponding mutation rule for the cluster variables, eq. (2.2), is invariant under this sign change, the latter equation then simplifies to the form (1.2) we stated in the introduction.

As the cluster algebras in question are finite, starting with the initial cluster $\{a_1, a_2\}$ and performing mutations generates a finite number of distinct clusters and variables, after which we land back to the initial cluster. In the $L = 2$ or C_2 case the collection of distinct cluster variables from all clusters yields the set quoted in eq. (1.3), and similarly in the $L = 3$ or G_2 case we obtain,

$$\Phi_{G_2} = \left\{ a_1, a_2, \frac{1+a_2^3}{a_1}, \frac{1+a_1+a_2^3}{a_1 a_2}, \frac{1+a_1^3+3a_1^2+3a_1 a_2^3+3a_1+a_2^6+2a_2^3}{a_1^2 a_2^3}, \frac{1+a_1^2+2a_1+a_2^3}{a_1 a_2^2}, \right.$$
$$\left. \frac{1+a_1^3+3a_1^2+3a_1+a_2^3}{a_1 a_2^3}, \frac{1+a_1}{a_2} \right\}. \tag{2.6}$$

The colour-coding is explained as follows: the subset of cyan variables is multiplicatively equivalent to the A_2 cluster variables after the replacement

$$a_2 \to a_2^{1/3}\,, \tag{2.7}$$

or in other words the logarithms of the variables span the same linear space.[3] Similarly, by adding the blue variable to them one obtains a subset that is multiplicatively equivalent to the C_2 cluster algebra after the replacement

$$a_2 \to a_2^{2/3}\,. \tag{2.8}$$

More explicitly, by dropping the purely G_2 violet variables and using (2.8) in eq. (2.6), it is easy to check that the numerators of the remaining variables match (up to overall rational exponents) those of eq. (1.3).

Apart from the cluster variables per se, we will also be interested in how these arrange themselves into clusters. This information is visualised in the exchange graph, as defined in the previous subsection, and which for the case of G_2 is depicted in figure 2. The fact that the C_2 and A_2 cluster variables are contained, up to multiplicative equivalence, in G_2, induces a relation between the two cluster algebras also at the level of their exchange graphs: the C_2 exchange graph can be obtained from the G_2 one by dropping any purely G_2 variable as well as contracting the edges of the two clusters containing it, and similarly for A_2.

From the exchange graph we may also easily infer that the G_2 cluster variable a_i may be found together with a_{i-1} and a_{i+1} in some cluster. This is precisely the information encoded in the notion of the neighbour set also defined at the end of the previous section, which in this case reads,

$$ns_{G_2}(a_i) = \{a_{i-1}, a_i, a_{i+1}\} \quad i = 1, \ldots, 8. \tag{2.9}$$

[3] As will be elaborated on below, polylogarithmic function spaces with cluster variables as letters are defined up to this equivalence, hence our interest in it.

JHEP01(2025)197

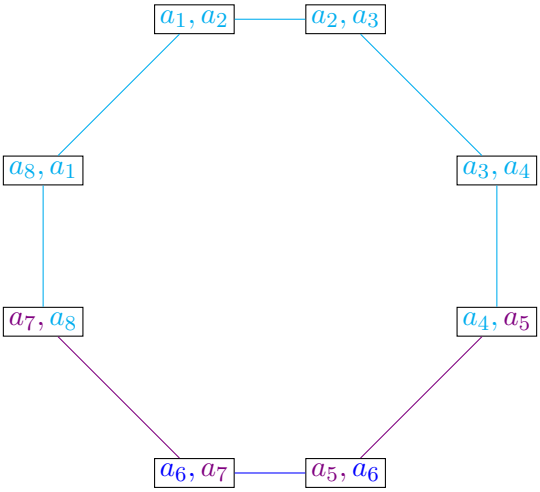

Figure 2. Exchange graph of the G_2 cluster algebra, with the expressions for the letters a_i given in eq. (2.6) in the order they appear. Removing a_5, a_7 (and a_6) and fusing the clusters containing them essentially yields the C_2 (A_2) cluster algebra, as discussed in the text.

2.3 Folded cluster algebras and embedded neighbour sets

Every non-simply laced Lie algebra, or its corresponding Dynkin diagram, may be obtained from a simply laced one from a procedure known as *folding*. In particular, we have

$$\begin{aligned} A_{2n-1} &\to C_n\,, \quad D_4 \to G_2\,, \\ D_{n+1} &\to B_n\,, \quad E_6 \to F_4\,, \end{aligned} \tag{2.10}$$

and the same procedure also carries over to the associated cluster algebras [31].[4] Conversely, this provides an embedding of a skew-symmetrisable cluster algebra inside a larger cluster algebra. We will make use of this type of embedding for G_2 in subsection 4.2, where we will see that it has implications for the adjancency relations of the form (1.4) for the differential equations of the three-loop nonplanar ladder integral.

In the rest of this subsection, we review how to fold cluster algebras, also using the $A_3 \to C_2$ example to illustrate the general process. We will also show how folding naturally extends the notion of neighbour sets to *embedded neighbour sets*, see in particular Definition 1 below. The reader interested primarily in the cluster-algebraic structure of alphabets, rather than of adjacency relations, may thus choose to directly skip to the next section.

At the level of Dynkin diagrams, folding may be thought of as an identification between different nodes that are mapped into each other by an (outer automorphism) symmetry leaving the entire diagram invariant. At the level of a cluster algebra, this symmetry is in turn with respect to permutations of the rows of the exchange matrix;[5] Folding of the cluster algebra essentially amounts to equating the cluster variables associated to the rows in question, and only considering simultaneous mutations of these variables (and usual mutations of the rest) [83].

[4] From the relation (2.3) between Cartan and exchange matrices, it also follows that (non-)simply laced Lie algebras are associated to skew-symmetric (skew-symmetrisable) cluster algebras.

[5] As the exchange matrix we begin with is skew-symmetric, also its columns will respect the same symmetry.

JHEP01(2025)197

In this manner, one produces the subset of the seeds of the skew-symmetric cluster algebra, whose exchange matrix will respect an analogous permutation symmetry. As a consequence, these clusters will also have the same number of cluster variables equal after the aforementioned replacement, and we may use the count of distinct variables as a criterion to select the subset in question when starting from the entire skew-symmetric cluster algebra. Furthermore, from the cluster variable mutation rule (2.2), it is evident that

$$a_i^{[\pm b_{ik}]_+} a_j^{[\pm b_{jk}]_+} \xrightarrow{a_j = a_i} a_i^{[\pm b_{ik}]_+ + [\pm b_{jk}]_+} . \tag{2.11}$$

In other words, the identification of two cluster variables implies that their corresponding rows in the exchange matrix need to be replaced by the sum of the two, also appropriately eliminating rows so as to end up with a rectangular matrix. All in all, from these considerations we obtain the following general folding procedure.

Folding cluster algebras:

1. Start with a skew-symmetric ADE cluster algebra appearing on the left of any arrow in eq. (2.10), and pick a seed whose exchange matrix is symmetric under a certain permutation of its rows.

2. Equate the cluster variables related by this permutation, and select the subset of all clusters containing the same numbers of equal cluster variables.

3. In each of the selected clusters, for each collection of equal cluster variables, replace the corresponding rows of the exchange matrix with a single row summing them up. Eliminate the columns of the matrix as well as the duplicate cluster variables having the same position as the eliminated rows.

4. The seeds thus obtained are seeds of the skew-symmetrisable cluster algebra at the other end of the arrow in eq. (2.10).

Let us see this procedure at work in the example of $A_3 \to C_2$ folding. We start with the A_3 seed with cluster variables and exchange matrix, respectively,

$$\{a_0, a_1, a_2\}\,, \quad \bar{B} = \begin{bmatrix} 0 & -1 & 0 \\ 1 & 0 & 1 \\ 0 & -1 & 0 \end{bmatrix}\,, \tag{2.12}$$

and for our purposes it will be sufficient to consider two more seeds of the cluster algebra,

$$\left\{\frac{1+a_1}{a_0}, a_1, a_2\right\}\,, \qquad \bar{B}' = \begin{bmatrix} 0 & 1 & 0 \\ -1 & 0 & 1 \\ 0 & -1 & 0 \end{bmatrix}\,, \tag{2.13}$$

$$\left\{\frac{1+a_1}{a_0}, a_1, \frac{1+a_1}{a_2}\right\}\,, \qquad \bar{B}'' = \begin{bmatrix} 0 & 1 & 0 \\ -1 & 0 & -1 \\ 0 & 1 & 0 \end{bmatrix}\,, \tag{2.14}$$

JHEP01(2025)197

obtained by mutating first a_0 and then a_2 in (2.12). The matrix $\bar{B}$ in the latter formula is symmetric under the exchange of the first and third row and column, so according to step 2 above we may set $a_0 = a_2$. This renders equal two cluster variables not only in this seed but also in the seed of eq. (2.14), and so we select these seeds. On the contrary the three cluster variables of the seed (2.13) remain distinct and so we discard it (also notice that, unlike the two seeds we selected, the exchange matrix of this seed does not have a permutation symmetry).

We now proceed to produce the C_2 seeds corresponding to eqs. (2.12) and (2.14) by identifying the equal cluster variables as described in step 3 above. In both selected clusters the permutation symmetry is with respect to the first and third row, and we may choose to replace the latter with the sum of the two. This eliminates the first row, and consequently also the first column of the matrix, as well as the first cluster variable. Therefore folding eqs. (2.12) and (2.14) yields

$$\{a_1, a_2\}\,, \qquad B = \begin{bmatrix} 0 & 1 \\ -2 & 0 \end{bmatrix}\,, \tag{2.15}$$

$$\left\{a_1, \frac{1+a_1}{a_2}\right\}\,, \qquad B'' = \begin{bmatrix} 0 & -1 \\ 2 & 0 \end{bmatrix}\,, \tag{2.16}$$

respectively, and it's easy to show that both are indeed seeds of the C_2 cluster algebra: the first of the above equations is nothing but the C_2 initial seed with an exchange matrix equal to eq. (2.4) with $L = 2$, whereas the second equation the seed obtained by mutating a_2 in the former.

Similarly, carrying out this procedure for all 14 of the A_3 seeds selects 6 of them, which are found to be equal to the C_2 seeds as expected by the coarsening of the G_2 exchange graph shown in figure 2. It also follows that the set of cluster variables of the folded cluster algebra is directly obtained from that of the unfolded cluster algebra we begin with, after the variable identification discussed in step 2 above. For the A_3 example at hand, it is in particular simple to check that its set of cluster variables,

$$\left\{a_0, a_1, a_2, \frac{1+a_1}{a_0}, \frac{1+a_0a_2}{a_1}, \frac{1+a_1}{a_2}, \frac{1+a_1+a_0a_2}{a_0a_1}, \frac{1+a_1+a_0a_2}{a_1a_2}, \frac{1+2a_1+a_1^2+a_0a_2}{a_0a_1a_2}\right\}\,,$$

indeed reduces to that of C_2, eq. (1.3), after the $A_3 \to C_2$ folding replacement $a_0 = a_2$ and the elimination of duplicate elements.

Before concluding this section, let us present a final related concept that will be very useful when analysing adjacency relations in section 4. As the folding procedure we have described may be thought of as an embedding of a skew-symmetrisable cluster algebra inside a larger cluster algebra, it also allows us to generalise the notion of the neighbour set defined at the end of subsection 2.1, and also illustrated in the example of the G_2 cluster algebra in eq. (2.9). Namely, cluster variables that do not appear together in clusters of the folded cluster algebra, may appear together in clusters of the larger cluster algebra containing it. This gives rise to the notion of an *embedded neighbour set*, which may be formally defined as follows.

Definition 1 (Embedded neighbour set) *Let $a_i \in A$ and $f_i \in F$ be cluster variables of two cluster algebras related by folding $A \to F$, which in particular equates $a_j = f_i$ for some*

JHEP01(2025)197

indices j and all indices i. Then the embedded neighbour set of $F \subset A$ is given by

$$ns_{F\subset A}(f_i) = \bigcup_j ns_A(a_j)\Big|_{a_j=f_i} . \tag{2.17}$$

In other words, we first compute the neighbour sets for the variables of the cluster algebra A, and then set some of them equal, as dictated by folding. For the subset of variables that become equal to the cluster variables of F after this replacement, we take the union of their neighbour sets, where the same replacement is also applied.

To make the embedded neighbour set definition more transparent, we apply it to our $A_3 \to C_2$ example. The A_3 neighbour sets are,

$$\begin{aligned}
ns_{A_3}(a_0) &= \left\{a_0, a_1, a_2, \frac{1+a_1}{a_2}, \frac{1+a_0a_2}{a_1}, \frac{1+a_1+a_0a_2}{a_1a_2}\right\},\\
ns_{A_3}(a_1) &= \left\{a_0, a_1, a_2, \frac{1+a_1}{a_0}, \frac{1+a_1}{a_2}\right\},\\
ns_{A_3}(a_2) &= \left\{a_0, a_1, \frac{1+a_1}{a_0}, a_2, \frac{1+a_0a_2}{a_1}, \frac{1+a_1+a_0a_2}{a_0a_1}\right\},\\
ns_{A_3}\left(\frac{1+a_1}{a_0}\right) &= \left\{a_1, \frac{1+a_1}{a_0}, \frac{1+a_1}{a_2}, a_2, \frac{1+a_1+a_0a_2}{a_0a_1}, \frac{1+2a_1+a_1^2+a_0a_2}{a_0a_1a_2}\right\},\\
ns_{A_3}\left(\frac{1+a_0a_2}{a_1}\right) &= \left\{a_0, a_2, \frac{1+a_0a_2}{a_1}, \frac{1+a_1+a_0a_2}{a_0a_1}, \frac{1+a_1+a_0a_2}{a_1a_2}\right\},\\
ns_{A_3}\left(\frac{1+a_1}{a_2}\right) &= \left\{a_0, a_1, \frac{1+a_1}{a_0}, \frac{1+a_1}{a_2}, \frac{1+a_1+a_0a_2}{a_1a_2}, \frac{1+2a_1+a_1^2+a_0a_2}{a_0a_1a_2}\right\},\\
ns_{A_3}\left(\frac{1+a_1+a_0a_2}{a_0a_1}\right) &= \left\{\frac{1+a_1}{a_0}, a_2, \frac{1+a_0a_2}{a_1}, \frac{1+a_1+a_0a_2}{a_0a_1}, \frac{1+a_1+a_0a_2}{a_1a_2}, \frac{1+2a_1+a_1^2+a_0a_2}{a_0a_1a_2}\right\},\\
ns_{A_3}\left(\frac{1+2a_1+a_1^2+a_0a_2}{a_0a_1a_2}\right) &= \left\{\frac{1+a_1}{a_0}, \frac{1+a_1}{a_2}, \frac{1+a_1+a_0a_2}{a_0a_1}, \frac{1+a_1+a_0a_2}{a_1a_2}, \frac{1+2a_1+a_1^2+a_0a_2}{a_0a_1a_2}\right\},\\
ns_{A_3}\left(\frac{1+a_1+a_0a_2}{a_2a_1}\right) &= \left\{a_0, \frac{1+a_1}{a_2}, \frac{1+a_0a_2}{a_1}, \frac{1+a_1+a_0a_2}{a_0a_1}, \frac{1+a_1+a_0a_2}{a_1a_2}, \frac{1+2a_1+a_1^2+a_0a_2}{a_0a_1a_2}\right\}.
\end{aligned} \tag{2.18}$$

Upon the identification $a_0 = a_2$ that performs the $A_3 \to C_2$ folding, two more pairs of cluster variables become equal to each other (those appearing on the left-hand side of lines 4-7 and 5-9 above). We observe that the neighbour sets of the cluster variables that are identified with each other also coincide, and altogether the $C_2 \subset A_3$ embedded neighbour sets thus become,

$$\begin{aligned}
ns_{C_2\subset A_3}(a_1) &= \left\{a_1, a_2, \frac{1+a_1}{a_2}\right\}\\
ns_{C_2\subset A_3}(a_2) &= \left\{a_1, a_2, \frac{1+a_1}{a_2}, \frac{1+a_2^2}{a_1}, \frac{1+a_1+a_2^2}{a_1a_2}\right\},\\
ns_{C_2\subset A_3}\left(\frac{1+a_2^2}{a_1}\right) &= \left\{a_2, \frac{1+a_2^2}{a_1}, \frac{1+a_1+a_2^2}{a_1a_2}\right\},\\
ns_{C_2\subset A_3}\left(\frac{1+a_1}{a_2}\right) &= \left\{a_1, a_2, \frac{1+a_1}{a_2}, \frac{1+a_1+a_2^2}{a_1a_2}, \frac{1+2a_1+a_1^2+a_2^2}{a_1a_2^2}\right\},\\
ns_{C_2\subset A_3}\left(\frac{1+2a_1+a_1^2+a_2^2}{a_1a_2^2}\right) &= \left\{\frac{1+a_1}{a_2}, \frac{1+a_1+a_2^2}{a_1a_2}, \frac{1+2a_1+a_1^2+a_2^2}{a_1a_2^2}\right\},\\
ns_{C_2\subset A_3}\left(\frac{1+a_1+a_2^2}{a_1a_2}\right) &= \left\{a_2, \frac{1+a_1}{a_2}, \frac{1+a_2^2}{a_1}, \frac{1+a_1+a_2^2}{a_1a_2}, \frac{1+2a_1+a_1^2+a_2^2}{a_1a_2^2}\right\}.
\end{aligned} \tag{2.19}$$

JHEP01(2025)197

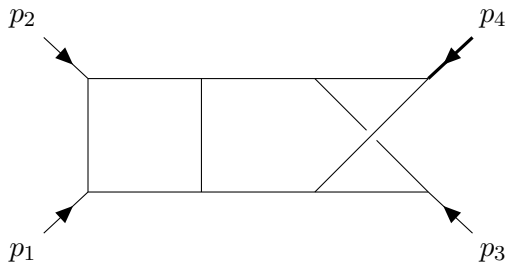

Figure 3. The B1 topology producing new letters.

Notice in particular that some of these neighbour sets are *larger* than the usual C_2 neighbour sets of the same cluster variables. Indeed the latter always contain three elements, as every C_2 cluster variable appears in two clusters related by a mutation.

3 Nonplanar 3-loop 1-mass Ladder: alphabet

Our goal will be to understand the cluster-algebraic structure of three-loop four-point integrals with one external leg offshell/massive, and everything else massless. Many integral families with these kinematics have been recently calculated in [67–70], and all of them continue to be described by a C_2 cluster algebra relevant at two loops [41], except the nonplanar topology shown in figure 3. As its alphabet contains that of all the other integrals, from now on we will thus restrict our attention to this nonplanar triple ladder.

We choose to label the external momenta as shown in the figure, with $p_1^2 = p_2^2 = p_3^2 = 0$ and $p_4^2 \neq 0$. The kinematic variables of the process are thus

$$s = (p_1 + p_2)^2, t = (p_1 + p_3)^2, p_4^2, \tag{3.1}$$

and, following the conventions of [69], the symbol alphabet for the canonical differential equations (1.1) of all currently known integrals with these kinematics is contained in

$$\mathbf{\Phi}_0 = \{\alpha_0, \alpha_1, \ldots, \alpha_8\} = \{p_4^2, s, t, -p_4^2 + s + t, -p_4^2 + s, s + t, -(p_4^2 - s)^2 + p_4^2 t, s^2 - p_4^2(s - t)\}. \tag{3.2}$$

Without loss of generality, we can always render the alphabet dimensionless by dividing out with one of the dimensionful letters, which is taken as the overall scale of the Feynman integral. In our case we will take this overall scale to be $\alpha_0 = p_4^2$, and in particular define the dimensionless version of the kinematic variables (3.1) as

$$z_1 = \frac{-s}{-p_4^2}, \quad z_2 = \frac{-t}{-p_4^2}. \tag{3.3}$$

The dimensionless alphabet in terms of these variables finally becomes,

$$\mathbf{\Phi} = \{z_1, z_2, 1 - z_1 - z_2, 1 - z_1, 1 - z_2, z_1 + z_2, 1 - 2z_1 + z_1^2 - z_2, z_1 - z_1^2 - z_2\}, \tag{3.4}$$

where we again use colour-coding to denote the letters that first appear at one, two and three loops.

We would like to explore whether the alphabet (3.4) has a cluster-algebraic interpretation. To this end, we will first need to review and refine the general framework for proving the equivalence of different sets of alphabets.

JHEP01(2025)197

3.1 General procedure for equivalence of alphabets

Our starting point is the well-known fact that under linear transformations of the form

$$d\log\alpha_i = \sum_j M_{ij}\, d\log\alpha'_j\,, \tag{3.5}$$

where M_{ij} are the elements of a square invertible rational matrix, the canonical differential equations (1.1) preserve their general form. Specifically, they transform to

$$d\mathbf{f}(\vec{z};\epsilon) = \epsilon \left[\sum_j \mathbf{A}'_j\, d\log\alpha'_j(\vec{z})\right] \mathbf{f}(\vec{z};\epsilon), \tag{3.6}$$

where

$$\mathbf{A}'_j = \sum_i \mathbf{A}_i M_{ij}\,. \tag{3.7}$$

Therefore, any two symbol alphabets $\{\alpha_i\}$ and $\{\alpha'_i\}$ are considered equivalent if they are related by a transformation of the form (3.5), or in other words alphabets are only defined up to the equivalence relation $\{\alpha_i\} \sim \{\alpha'_i\}$, rather than uniquely.

Provided the alphabets $\{\alpha_i\}$ and $\{\alpha'_i\}$ depend on the same variables $\vec{z}$, one may easily check if they are equivalent in a numerical fashion, see e.g. [84]: one forms the list

$$L(\vec{z}) = \{\log|\alpha_1(\vec{z})|, \ldots, \log|\alpha_N(\vec{z})|, \log|\alpha'_1(\vec{z})|, \ldots, \log|\alpha'_N(\vec{z})|\}\,, \tag{3.8}$$

where the absolute value is placed so as to throw away any sign information which is not relevant for symbol letters, and for definitiveness we have specified the size of the two alphabets to be N. Next, one evaluates this list for (at least) $2N$ random values of the variables, $\vec{z}^{(1)}, \ldots, \vec{z}^{(2N)}$, and from them constructs the matrix,

$$R = \begin{pmatrix} L(\vec{z}^{(1)}) \\ \vdots \\ L(\vec{z}^{(2N)}) \end{pmatrix}. \tag{3.9}$$

Then, checking whether the two alphabets are equivalent or not boils down to the computation of the rank of this matrix,

$$\mathrm{rank}(R) = N \quad \Leftrightarrow \quad \{\alpha_i\} \sim \{\alpha'_i\}\,. \tag{3.10}$$

More often, however, we are interested in comparing alphabets that depend on *different variables*, $\{\alpha_i(\vec{z})\}$, $\{\alpha'_i(\vec{z}')\}$. In other words, we also need to find the transformation

$$\vec{z}' = \vec{g}(\vec{z})\,, \tag{3.11}$$

so as to be able to carry out the equivalence test (3.8)–(3.10). The key idea here is that *if the variables $\vec{z}$ are themselves letters, then their general form is also constrained by eq.* (3.5).[6] If

[6]The requirement that the variables are themselves letters is not a limitation in practice, as we can always pick a subset of algebraically independent letters as variables.

JHEP01(2025)197

this requirement holds, and $\{\alpha_i\} \sim \{\alpha'_i\}$, then taking the exponential of the latter relation for the variables $\vec{z}$ yields,

$$z'_m \in \{\alpha'_i\} \quad \Rightarrow \quad z'_m = c_m \prod_{j=1}^{N} \alpha_j(\vec{z})^{n_{mj}}\,, \ m = 1, \ldots, d\,, \tag{3.12}$$

where for concreteness we have assumed that the number of independent variables of both alphabets is d, $\vec{z} = (z_1, \ldots, z_d)$ and similarly for the primed case.

The above formula equips us with a systematic way to establish the equivalence of two alphabets $\{\alpha_i(\vec{z})\}$, $\{\alpha'_i(\vec{z}')\}$, both having size N and d independent variables: we perform the transformation (3.12) on the alphabet $\{\alpha'_i(\vec{z}')\}$ for a range of different values c_m, n_{mj}, construct the matrix R as in eqs. (3.8)–(3.9) and compute its rank. Per eq. (3.10), if for certain values of c_m, n_{mj} this rank equals N, then these determine the transformation (3.11), and prove the equivalence of the two alphabets.

We may also drastically reduce the number of matrix rank evaluations of the method, and thereby achieve a corresponding improvement in its efficiency, as follows: assuming that we scan a range of r values for each n_{mj}, if we were to transform all z_m similtaneously the number of evaluations would be proportinal to $r^{d \cdot N}$. Instead, we *split the above computation into d smaller computations, one for each individual value of m in eq.* (3.12)*, where we also keep only the subset of single-variable letters $\{\alpha'_{i_1}(z'_m), \ldots, \alpha'_{i_K}(z'_m)\}$ in the second half of the list* (3.8). Each smaller computation will involve matrices R of size $N + K$ instead of $2N$, whose rank is thus also faster to evaluate, and the number of matrix rank evaluations of all of them together will now be proportional to $d \cdot r^N$ instead of $r^{d \cdot N}$. Finally, we form the complete list of the two alphabets L in eq. (3.8), and carry out the test (3.10), but now we scan only over the subset of c_m, n_{mj} values that have already passed the test in each of the smaller computations. Usually there's just a handful of such values, so this final step has negligible computational overhead.

Of course, if a variable transformation and alphabet equivalence is discovered numerically as described above, in the end it may also be checked analytically to further confirm its correctness. Input parameters of the method we have described include the ordering of the two alphabets, the range of values we scan for c_m, n_{mj}, the range and type of numbers (integer/rational/real) for the random kinematic points, as well as the numerical precision of the rank evaluation. Finally, it is worth noting that this method can also be straightforwardly generalised so as to also look for the inclusion of one alphabet inside the other.

3.2 Application: ladder alphabet = G_2 cluster algebra

We now move on to apply the general procedure we have described in the previous section, in order to investigate whether the alphabet (3.4) of the nonplanar triple ladder integral is equivalent to the G_2 cluster algebra alphabet (2.6): both have 8 letters and depend on two variables, which are necessary conditions for their equivalence. Furthermore, the variables z_1, z_2 are also letters of the former alphabet, such that our method can be applied directly.

For simplicity, instead of the G_2 alphabet (2.6) we choose the alphabet of its irreducible factors (the two are equivalent by virtue of eq. (3.5)) as our $\{\alpha'_i(a_1, a_2^3)\}$. Notice, in particular, that we pick a_2^3 instead of a_2 as a variable, since only the former appears in the irreducible

JHEP01(2025)197

factors. As the range of values for our scan we pick $c_m = \pm 1$ and $n_{mj} = \{-1, 0, 1\}$. Finally, we choose integer random kinematic points, and compute the rank with 100 digits of precision.

In this manner, we find the transformation

$$\begin{aligned} z_1 =& \frac{(1+a_1)(1+a_1+a_2^3)}{a_1 a_2^3}\,, \\ z_2 =& -\frac{1+a_1}{a_2^3}\,, \end{aligned} \tag{3.13}$$

and we also check analytically that it indeed proves the equivalence of the alphabets (3.4) and (2.6). Concretely, the letters of the former, nonplanar triple ladder alphabet in terms of the G_2 alphabet read,

$$\Phi = \left\{ \frac{a_4 a_8}{a_2}, -\frac{a_8}{a_2^2}, -\frac{a_4}{a_2^2}, -\frac{a_6}{a_2}, \frac{a_1 a_4}{a_2^2}, \frac{a_3 a_8}{a_2^2}, \frac{a_7 a_4}{a_2^2}, -\frac{a_5 a_8}{a_2^2} \right\}. \tag{3.14}$$

4 Nonplanar 3-loop 1-mass Ladder: adjacencies

4.1 Observed adjacency restrictions

In the previous section, we showed that the alphabet (3.4), controlling the three-loop one-mass nonplanar ladder integral, is equivalent to the one of eq. (2.6), dictated by the G_2 cluster algebra. That is, the former alphabet is related to the latter by a transformation of the form (3.5), and it is also interesting to investigate adjacency restrictions of the transformed coefficient matrices $\mathbf{A}'_i$ of this integral, eq. (3.7), in the G_2 alphabet.

We find that

$$\mathbf{A}'_i \cdot \mathbf{A}'_j = \mathbf{A}'_j \cdot \mathbf{A}'_i = 0 \;\text{ for }\; \begin{cases} i,j \in \{1,3,5,7\} & \text{with } i > j\,, \\ j = i+3\,, i = 3,\ldots,6 & \text{with } j \sim j-8\,, \end{cases}\,, \tag{4.1}$$

namely we obtain 12+8=20 adjacency restrictions. These contain the 6 restrictions observed previously for the C_2 subalphabet of G_2 [41], see also [85], plus another 14 relations involving either or both of the new, purely G_2 letters a_5, a_7 in eq. (2.6).

We note that 16 of these restrictions were visible in the original alphabet (3.4). Namely our cluster-algebraic analysis already has the benefit of revealing new adjacency restrictions, and in subsection 4.3 we will explore how such adjacency restrictions reduce the size of the relevant function space. To see how the new adjacency restrictions look like in the original alphabet (3.4) of the nonplanar 3-loop 1-mass ladder, we first reexpress the relation (3.14) between these letters and those of the G_2 alphabet in the form (3.5), and read off the corresponding transformation matrix M. Plugging this in eq. (3.7), we find that the primed coefficient matrices in the G_2 alphabet are related to those of the original reference [69] by,

$$\mathbf{A}'_1 = \mathbf{A}_5\,, \qquad \mathbf{A}'_3 = \mathbf{A}_6\,, \qquad \mathbf{A}'_5 = \mathbf{A}_8,\,, \qquad \mathbf{A}'_6 = \mathbf{A}_4\,, \qquad \mathbf{A}'_7 = \mathbf{A}_7 \tag{4.2}$$

$$\mathbf{A}_2 = -\mathbf{A}_1 - 2\mathbf{A}_2 - 2\mathbf{A}_3 - \mathbf{A}_4 - 2\mathbf{A}_5 - 2\mathbf{A}_6 - 2\mathbf{A}_7 - 2\mathbf{A}_8\,, \tag{4.3}$$

$$\mathbf{A}'_4 = \mathbf{A}_1 + \mathbf{A}_3 + \mathbf{A}_5 + \mathbf{A}_7\,, \qquad \mathbf{A}'_8 = \mathbf{A}_1 + \mathbf{A}_2 + \mathbf{A}_6 + \mathbf{A}_8\,. \tag{4.4}$$

Clearly, the subset of adjacency restrictions (4.1) where only matrices of eq. (4.2) participate, have precisely the same simple form in the original alphabet up to index relabellings, and

JHEP01(2025)197

correspond to the 16 visible relations we mentioned at the beginning of this paragraph. However the restrictions involving the matrices of eq. (4.4) become more complicated,

$$\begin{aligned}(\mathbf{A}_1+\mathbf{A}_3+\mathbf{A}_5+\mathbf{A}_7)\cdot\mathbf{A}_7=\mathbf{A}_7\cdot(\mathbf{A}_1+\mathbf{A}_3+\mathbf{A}_5+\mathbf{A}_7)=0\,,\\ \mathbf{A}_8\cdot(\mathbf{A}_1+\mathbf{A}_2+\mathbf{A}_6+\mathbf{A}_8)=(\mathbf{A}_1+\mathbf{A}_2+\mathbf{A}_6+\mathbf{A}_8)\cdot\mathbf{A}_8=0\,,\end{aligned} \tag{4.5}$$

and may thus only be found by simple inspection after our variable transformation, illustrating its advantage.

In $\mathcal{N}=4$ SYM theory, adjacency restrictions have been observed to be in 1-1 correspondence with the distribution of variables within clusters, encoded in their neighbour sets. In the language of canonical differential equations, this 'cluster adjacency' [71] correspondence could be stated as,

$$\mathbf{A}_i\cdot\mathbf{A}_j=\mathbf{A}_j\cdot\mathbf{A}_i=0 \quad\Leftrightarrow\quad \begin{array}{l}\nexists \text{ cluster containing } \alpha_i,\alpha_j\,,\\ \text{or equivalently } \alpha_i\notin ns(\alpha_j)\,.\end{array} \tag{4.6}$$

Note that for such cluster adjacency restrictions the order of the matrix product doesn't matter, since all statements on the right-hand side of the double arrow are independent of the order. Another way to say this, is that $\alpha_i\notin ns(\alpha_j)\Leftrightarrow\alpha_j\notin ns(\alpha_i)$.

This independence from the order of the matrix product is certainly something that our observed adjacencies (4.1) respect. But do they precisely match the $\mathcal{N}=4$ cluster adjacency predictions (4.6)? To answer this, we need to apply it to the G_2 neighbour sets, which we have presented in eq. (2.9). Since these contain three consecutive G_2 cluster variables, it follows that if $\mathcal{N}=4$ cluster adjacency were to hold, it would imply

$$\mathbf{A}'_i\cdot\mathbf{A}'_j\stackrel{?}{=}0 \quad \text{for } j\neq i,i\pm1\,, \tag{4.7}$$

namely 16+16+8=40 relations for $j=i\pm2$, $j=i\pm3$ and $j=i+4$, respectively.

Hence the $\mathcal{N}=4$ cluster adjacency predictions (4.7) don't match our observed adjacencies (4.1), though the latter are certainly contained in the former. A similar situation was also observed for the two-loop integrals for the same kinematics [41]. We can nevertheless aim to explain these by embedding the G_2 cluster algebras inside larger cluster algebras with the method of folding, reviewed together with the newly introduced concept of embedded neighbour pairs in section 2.3. The main idea is that since the larger cluster algebra contains more clusters, the neighbour sets of the G_2 variables inside of it will also become bigger, such that their complements, the $\mathcal{N}=4$ cluster adjacency restrictions (4.7), will reduce in number, and may approach or coincide with the observed adjacencies (4.1).

4.2 Intepretation by embedding G_2 inside D_4/B_3 cluster algebras

In section 2.3, we have recalled that both the G_2 and the B_3 cluster algebras can be embedded in the larger D_4 cluster algebra with the method of folding. As we will explain below, due to their common ancestry, G_2 may also be considered as part of the B_3 cluster algebra, and this relation is visualised in figure 4. Per Definition 1, we find that in both B_3 and D_4 embeddings of G_2 the corresponding neighbour sets become,

$$\begin{aligned}ns(a_1)_{G_2\subset D_4}=ns(a_1)_{G_2\subset B_3}=&\{a_8,a_1,a_2\}\,,\\ ns(a_2)_{G_2\subset D_4}=ns(a_2)_{G_2\subset B_3}=&\{a_1,a_2,a_3,a_4,a_6,a_8\}\,,\end{aligned} \quad + \quad a_i\to a_{i+2}\,, \tag{4.8}$$

JHEP01(2025)197

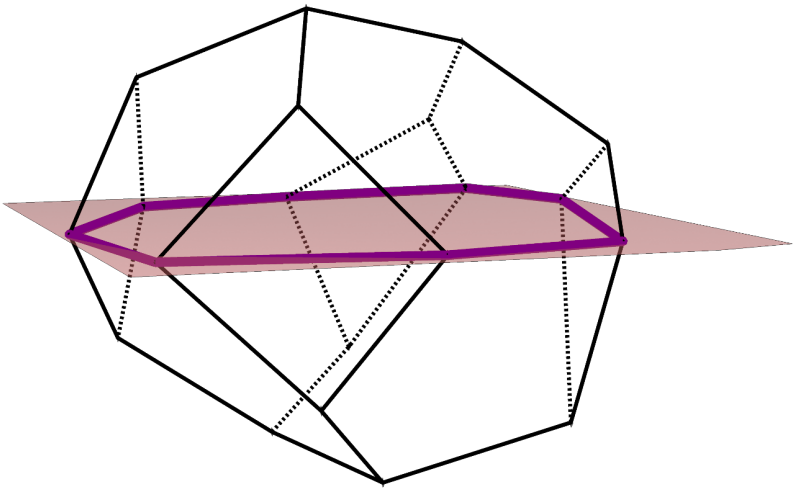

Figure 4. The three-dimensional cyclohedron with four square, four pentagonal and four hexagonal faces is the exchange graph of the B_3 cluster algebra. The G_2 exhange graph of figure 2 may be realised as a two-dimensional subspace thereof.

where cyclic identification of the cluster variable indices is implied. Compared to the G_2 neighbour sets (4.1) we notice that for the variables with odd indices a_{2j-1} they remain the same, but for the variables with even indices a_{2j} they double in size!

As a consequence, the embedding reduces the complement of the G_2 neighbour sets, the naive $\mathcal{N}=4$ cluster adjacency predictions (4.7) from 40 to 20+8=28 relations. Specifically, it eliminates the following 12 of the restrictions of eq. (4.7),

$$\cancel{\mathbf{A}'_{2i}\cdot\mathbf{A}'_{2j}=0}\,, \quad i\neq j=1,\ldots,4\,, \tag{4.9}$$

which the nonplanar triple ladder integral indeed does not obey. On the other hand, the embedding of G_2 inside the B_3 or D_4 cluster algebras still predicts that the restrictions of the second case in eq. (4.1) should hold for the entire range of $i=1,\ldots 8$, whereas the integral obeys only half of these mixed odd/even index restrictions, for $i=3,\ldots 6$. In any case, we find it encouraging that the embedding procedure we have described modifies the naive $\mathcal{N}=4$ cluster adjacency predictions (4.7) such that they approach the observed adjacency restrictions of the integral, and it would be interesting to explore if more general embeddings that go beyond what can be achieved by folding could also lead to a precise match.

In the rest of this subsection, we provide more details on how the result (4.8) was obtained. This closely mirrors the $A_3\to C_2$ folding example provided in subsection (2.3). A choice for the cluster variables and exchange matrix of the D_4 initial seed is

$$\{d_1,d_2,d_3,d_4\}\,, \quad B_{D_4}=\begin{bmatrix}0&-1&0&0\\1&0&1&1\\0&-1&0&0\\0&-1&0&0\end{bmatrix}\,, \tag{4.10}$$

which clearly is symmetric in the permutation of any of the rows 1,3,4. Following the folding procedure we described with respect to the first and fourth row, specifically eliminating the

JHEP01(2025)197

latter and the corresponding variable $d_4 \to d_1$, yields the B_3 seed

$$\{d_1, d_2, d_3\}\,, \quad B_{B_3} = \begin{bmatrix} 0 & -2 & 0 \\ 1 & 0 & 1 \\ 0 & -1 & 0 \end{bmatrix}\,. \tag{4.11}$$

Similarly, applying the same procedure for all rows 1,3,4, and in particular eliminating the latter two and their corresponding variables $d_4, d_3 \to d_1$, leads to the G_2 seed

$$\{d_1, d_2\}\,, \quad B_{G_2} = \begin{bmatrix} 0 & -3 \\ 1 & 0 \end{bmatrix}\,. \tag{4.12}$$

Indeed, the above exchange matrix is equivalent to the G_2 exchange matrix of eq. (2.4) with $L = 3$ up to a simultaneous reordering of rows and columns, which in turn amounts to an immaterial reordering of the variables of the cluster. In other words, one simply needs to relabel

$$d_1 \to a_2\,, d_2 \to a_1\,. \tag{4.13}$$

in order to match our previous conventions for the G_2 cluster algebra, as e.g. in eq. (2.6) and figure 2.

Notice that the G_2 seed (4.12) may alternatively be obtained by folding the B_3 seed (4.11), adding the third to the first column and eliminating $d_3 \to d_1$. It is in this sense that G_2 is also contained in B_3 as depicted in figure 4. Because the B_3 case is simpler, we will thus present the calculation of the embedded neighbour sets of G_2 with respect to the latter, only commenting on where the D_4 case differs.

The B_3 cluster algebra has 12 variables distributed to 20 clusters. Starting from the initial seed (4.11), and mutating according to the rules (2.1)–(2.2), in our ordering conventions the cluster variables read,

$$\begin{aligned} \Phi_{B_3} = \Bigg\{ & d_1, d_2, d_3, \frac{d_2+1}{d_1}, \frac{d_3 d_1^2+1}{d_2}, \frac{d_2+1}{d_3}, \frac{d_3 d_1^2 + d_2^2 + 2d_2 + 1}{d_1^2 d_2}, \frac{d_3 d_1^2 + d_2 + 1}{d_2 d_3}, \\ & \frac{d_3 d_1^2 + d_2 + 1}{d_1 d_2}, \frac{d_2^3 + 3d_2^2 + 3d_2 + d_1^2 d_3 + 1}{d_1^2 d_2 d_3}, \\ & \frac{d_3^2 d_1^4 + 3d_2 d_3 d_1^2 + 2d_3 d_1^2 + d_2^3 + 3d_2^2 + 3d_2 + 1}{d_1^2 d_2^2 d_3}, \frac{d_3 d_1^2 + d_2^2 + 2d_2 + 1}{d_1 d_2 d_3} \Bigg\} \equiv \{d_i\}_{i=1}^{12}\,, \end{aligned} \tag{4.14}$$

JHEP01(2025)197

whereas their neighbour sets are given by,

$$\begin{aligned}
ns_{B_3}(d_1) &= \{d_1, d_2, d_3, d_5, d_6, d_8\}\ , \\
ns_{B_3}(d_2) &= \{d_1, d_2, d_3, d_4, d_6\}\ , \\
ns_{B_3}(d_3) &= \{d_1, d_2, d_3, d_4, d_5, d_7, d_9\}\ , \\
ns_{B_3}(d_4) &= \{d_4, d_2, d_3, d_6, d_7, d_{10}\}\ , \\
ns_{B_3}(d_5) &= \{d_1, d_5, d_3, d_8, d_9\} \\
ns_{B_3}(d_6) &= \{d_1, d_2, d_6, d_4, d_8, d_{10}, d_{12}\}\ , \\
ns_{B_3}(d_7) &= \{d_4, d_7, d_3, d_9, d_{10}, d_{11}, d_{12}\}\ , \\
ns_{B_3}(d_8) &= \{d_1, d_5, d_8, d_6, d_9, d_{12}, d_{11}\}\ , \\
ns_{B_3}(d_9) &= \{d_5, d_9, d_3, d_7, d_8, d_{11}\}\ , \\
ns_{B_3}(d_{10}) &= \{d_4, d_{10}, d_6, d_7, d_{12}\}\ , \\
ns_{B_3}(d_{11}) &= \{d_9, d_{11}, d_7, d_8, d_{12}\}\ , \\
ns_{B_3}(d_{12}) &= \{d_8, d_{12}, d_6, d_{10}, d_{11}, d_7\}\ .
\end{aligned} \tag{4.15}$$

As mentioned already, the G_2 cluster algebra in our conventions is obtained from B_3 by the replacement $d_3 \to d_1$, together with the relabeling (4.13). For the entire set of B_3 variables, this implies

$$\begin{aligned}
&d_1, d_3 \to a_2\,, \qquad d_2 \to a_1\,, \quad d_4, d_6 \to a_8\,, \quad d_5 \to a_3\,, \\
&d_7, d_{12} \to a_6\,, \quad d_8, d_9 \to a_4\,, \qquad d_{10} \to a_7\,, \quad d_{11} \to a_5.
\end{aligned} \tag{4.16}$$

According to definition 1, in order to obtain the embedded neighbour set of a given G_2 variable, we need to take the union of the neighbour sets of all B_3 variables that reduce to it under the folding (4.16). For example, only d_2 reduces to a_1, and thus applying the replacement (4.16) to its neighbour set in (4.15) gives,

$$ns(a_1)_{G_2 \subset B_3} = \{a_1, a_2, a_8\}\,. \tag{4.17}$$

On the other hand both d_1 and d_3 reduce to a_2, so in order to compute its embedded neighbour set one needs to perform the replacement (4.16) on the union of the neighbour sets of the two B_3 variables, thus obtaining

$$ns(a_2)_{G_2 \subset B_3} = \{a_1, a_2, a_3, a_4, a_6, a_8\}\,. \tag{4.18}$$

Both of the last two formulas agree with what we already presented in (4.8), and the calculation proceeds also for the other neighbour sets in a similar fashion. Embedding G_2 inside D_4 also yields the same final result; the only difference in intermediate stages, is that the neighbour sets of D_4 variables that reduce to the same G_2 variables, also coincide.

4.3 Adjacent G_2 polylogarithmic function counts

Let us close this section by analysing the extent to which the adjacency restrictions (4.1), that we have discovered for the three-loop nonplanar ladder integral, reduce the size of the relevant

JHEP01(2025)197

Weight	1	2	3	4	5	6	7
No condition	8	46	232	1093	4944	21790	-
First entry	3	14	61	262	1113	4700	19755
Adjacency	3	14	54	196	684	2326	7796

Table 1. Dimension of the G_2 cluster function spaces (modulo transcendental constants) before and after constraints.

function space. In other words, we will construct the space of polylogarithmic functions of (transcendental) weight w, satisfying the defining property,

$$\mathrm{d}f^{(w)} = \sum_i f_i^{(w-1)} \mathrm{d}\log a_i, \tag{4.19}$$

where $f_i^{(w-1)}$ are weight-$(w-1)$ functions of the same type (with the recursion terminating with rational constants of weight 0 on the right-hand side) and a_i are the symbol letters, which in our case coincide the G_2 cluster variables (2.6).

At weight w, this function space will contain the $\mathcal{O}(\epsilon^w)$ term in the expansion of all currently computed four-point one-mass integrals, when normalised such that this expansion starts at $\mathcal{O}(\epsilon^0)$. First constructing this space and then seeking to identify the integrals or even directly the physical quantities they contribute to, is at the heart of the perturbative analytic bootstrap programme for scattering amplitudes and beyond, see [55] for a recent review. The success of this programme hinges on controlling the dimension of the function space at each weight, such that its construction is computationally feasible, and that the integral or physical quantity can be identified uniquely inside of it.

First of all, the dimension of the G_2 polylogarithmic function space at weight w will not be 8^w, because well-defined functions obey the property that double derivatives should yield the same result irrespective of the order of differentiation. This requirement is equivalent to the *integrability condition*,

$$\mathrm{d}^2 f^{(w)} = 0 \to \sum_i df_i^{(w-1)} \wedge \mathrm{d}\log a_i = 0\,, \tag{4.20}$$

which only allows particular weight-$(w-1)$ functions to appear on the right-hand side of eq. (4.19). The construction of integrable polylogarithmic functions modulo transcendental constants, also known as symbols, has been automated in the `Mathematica` package `SymBuild` [86], and applying it to our case yields the function counts shown on the first line of table 1.

Then, a necessary condition such that the produced functions have physical branch cuts, as dictated by locality and unitarity, is the *first entry condition*: the weight-one space must only contain letters that are Mandelstam variables. In the dimensionless alphabet of eq. (3.4), these correspond to the first three entries, and because of eq. (3.14) this is also equivalent to,

$$\text{First entry condition: } \vec{f}^{(1)} = \{\log z_1, \log z_2, \log(1-z_1-z_2)\} \sim \{\log a_2, \log a_4, \log a_8\}. \tag{4.21}$$

JHEP01(2025)197

The function counts when the first entry condition is additionally imposed are shown in the second line of table 1.[7]

Finally, on top of integrability and the first entry condition, we may also impose the additional adjacency restrictions (4.1), with the corresponding function space dimensions shown in the third line of table 1. We notice that they start having an effect already at weight 3, and that by weight 6 they have reduced the size of the integrable G_2 functions obeying just the first entry condition by more than a half. These results provide strong indications that such adjacency restrictions may play an important role in future extensions of the bootstrap programme to four-point one mass integrals or Higgs plus jet amplitudes in the heavy-top limit.

5 Conclusions and outlook

We have demonstrated that all four-point one-mass master integrals through three loops computed to date are governed by a G_2 cluster algebra, enlarging the C_2 cluster algebra previously seen to be relevant at two loops. In particular, the alphabet (3.1) entering their canonical differential equations (1.1) was shown to be equivalent to the set of G_2 cluster variables (2.6) thanks to the variable transformation (3.13). We find it remarkable that the A_2, C_2 and G_2 cluster algebras start becoming relevant at $L = 1, 2$ and 3 loops, respectively!

Focusing on the single integral with letters beyond those contained in the C_2 cluster algebra, shown in figure 3, we also looked for adjacency restrictions of the form $\mathbf{A}_i \cdot \mathbf{A}_j = 0$ for the constant matrices entering the canonical differential equations. We discovered that using the G_2 cluster variable form of the alphabet reveals new adjacency restrictions, yielding a total of 20 instead of the 16 that were visible in the original alphabet. While the observed adjacency restrictions do not coincide with the naive G_2 cluster adjacency expectations seen to hold in $\mathcal{N} = 4$ SYM theory, we showed that the two can be further aligned by embedding G_2 inside the larger B_3 or D_4 cluster algebras. We also illustrated the power of the adjacency restrictions we have observed by constructing the G_2 polylogarithmic function space, and noting that additionally imposing them leads to a significant reduction of its size.

Our work opens many exciting avenues for future inquiry. It would be very interesting to understand how the pattern of relevant cluster algebras continues for the complete set of master integrals at three as well as at higher loops, possibly entering the realm of infinite cluster algebras and the need to tame their infinite in a physically sensible manner, as was done in the case of cluster alphabets of $\mathcal{N} = 4$ SYM amplitudes [35–39]. With respect to adjacency restrictions, in [69] it was pointed out that one of the tennis-court four-point one-mass master integrals, while still described by the C_2 alphabet, does not respect the subset of the observed adjacencies (4.1) when restricted to this subalphabet. The authors of [87] comment that Schubert analysis can be used to determine certain letters appearing in four-point one-mass master integrals, so it would be worthwhile to investigate if it could also provide any insight on

[7] Note that the first entry condition is necessary but not sufficient condition for ensuring physical branch cuts. For the subspace of functions relevant for stress-tensor multiplet form factors in $\mathcal{N} = 4$ SYM theory, sufficient conditions were given in [85], and were shown to further reduce the number of functions modulo transcendental constants. As our focus is to gauge the power of the adjacency restrictions (4.1), we will not consider such additional constraints here.

JHEP01(2025)197

adjacency restrictions. More importantly, could the cluster-algebraic structure of alphabets and adjacency restrictions be deduced from first principles, and employed to make new predictions? Recent progress on efficient methods for computing the Landau singularities of Feynman integrals [88–91], and for also extracting symbol letters from them [92] or by related means [93–96], makes us optimistic that this ambitious endeavour is within reach.

Acknowledgments

We'd like to thank William Torres Bobadilla for stimulating discussions. RA and GP acknowledge support from the Deutsche Forschungsgemeinschaft (DFG) under Germany's Excellence Strategy – EXC 2121 "Quantum Universe" – 390833306. GP's work was supported in part by the UK Science and Technology Facilities Council grant ST/Z001021/1 and by the Munich Institute for Astro-, Particle and BioPhysics (MIAPbP) which is funded by the DFG under Germany's Excellence Strategy – EXC-2094 – 390783311.

Data Availability Statement. This article has no associated data or the data will not be deposited.

Code Availability Statement. This article has no associated code or the code will not be deposited.

References

[1] A. Huss, J. Huston, S. Jones and M. Pellen, *Les Houches 2021 — physics at TeV colliders: report on the standard model precision wishlist*, *J. Phys. G* **50** (2023) 043001 [arXiv:2207.02122] [INSPIRE].

[2] K.G. Chetyrkin and F.V. Tkachov, *Integration by parts: the algorithm to calculate β-functions in 4 loops*, *Nucl. Phys. B* **192** (1981) 159 [INSPIRE].

[3] A.V. Kotikov, *Differential equations method: new technique for massive Feynman diagrams calculation*, *Phys. Lett. B* **254** (1991) 158 [INSPIRE].

[4] E. Remiddi, *Differential equations for Feynman graph amplitudes*, *Nuovo Cim. A* **110** (1997) 1435 [hep-th/9711188] [INSPIRE].

[5] T. Gehrmann and E. Remiddi, *Differential equations for two-loop four-point functions*, *Nucl. Phys. B* **580** (2000) 485 [hep-ph/9912329] [INSPIRE].

[6] J.M. Henn, *Multiloop integrals in dimensional regularization made simple*, *Phys. Rev. Lett.* **110** (2013) 251601 [arXiv:1304.1806] [INSPIRE].

[7] K.-T. Chen, *Iterated path integrals*, *Bull. Am. Math. Soc.* **83** (1977) 831 [INSPIRE].

[8] A.B. Goncharov, *Multiple polylogarithms and mixed Tate motives*, math/0103059 [INSPIRE].

[9] A.B. Goncharov, *Galois symmetries of fundamental groupoids and noncommutative geometry*, *Duke Math. J.* **128** (2005) 209 [math/0208144] [INSPIRE].

JHEP01(2025)197

[10] A.B. Goncharov, M. Spradlin, C. Vergu and A. Volovich, *Classical Polylogarithms for Amplitudes and Wilson Loops*, *Phys. Rev. Lett.* **105** (2010) 151605 [arXiv:1006.5703] [INSPIRE].

[11] S. Abreu et al., *All Two-Loop Feynman Integrals for Five-Point One-Mass Scattering*, *Phys. Rev. Lett.* **132** (2024) 141601 [arXiv:2306.15431] [INSPIRE].

[12] S. Abreu, B. Page and M. Zeng, *Differential equations from unitarity cuts: nonplanar hexa-box integrals*, *JHEP* **01** (2019) 006 [arXiv:1807.11522] [INSPIRE].

[13] S. Fomin and A. Zelevinsky, *Cluster algebras I: foundations*, *Journal of the American Mathematical Society* **15** (2001) 497 [math/0104151] [INSPIRE].

[14] J. Golden et al., *Motivic Amplitudes and Cluster Coordinates*, *JHEP* **01** (2014) 091 [arXiv:1305.1617] [INSPIRE].

[15] L.J. Dixon, J.M. Drummond and J.M. Henn, *Bootstrapping the three-loop hexagon*, *JHEP* **11** (2011) 023 [arXiv:1108.4461] [INSPIRE].

[16] L.J. Dixon, J.M. Drummond and J.M. Henn, *Analytic result for the two-loop six-point NMHV amplitude in $N = 4$ super Yang-Mills theory*, *JHEP* **01** (2012) 024 [arXiv:1111.1704] [INSPIRE].

[17] L.J. Dixon, J.M. Drummond, M. von Hippel and J. Pennington, *Hexagon functions and the three-loop remainder function*, *JHEP* **12** (2013) 049 [arXiv:1308.2276] [INSPIRE].

[18] L.J. Dixon, J.M. Drummond, C. Duhr and J. Pennington, *The four-loop remainder function and multi-Regge behavior at NNLLA in planar $N = 4$ super-Yang-Mills theory*, *JHEP* **06** (2014) 116 [arXiv:1402.3300] [INSPIRE].

[19] L.J. Dixon and M. von Hippel, *Bootstrapping an NMHV amplitude through three loops*, *JHEP* **10** (2014) 065 [arXiv:1408.1505] [INSPIRE].

[20] J.M. Drummond, G. Papathanasiou and M. Spradlin, *A Symbol of Uniqueness: the cluster Bootstrap for the 3-Loop MHV Heptagon*, *JHEP* **03** (2015) 072 [arXiv:1412.3763] [INSPIRE].

[21] L.J. Dixon, M. von Hippel and A.J. McLeod, *The four-loop six-gluon NMHV ratio function*, *JHEP* **01** (2016) 053 [arXiv:1509.08127] [INSPIRE].

[22] S. Caron-Huot, L.J. Dixon, A. McLeod and M. von Hippel, *Bootstrapping a Five-Loop Amplitude Using Steinmann Relations*, *Phys. Rev. Lett.* **117** (2016) 241601 [arXiv:1609.00669] [INSPIRE].

[23] L.J. Dixon et al., *Heptagons from the Steinmann Cluster Bootstrap*, *JHEP* **02** (2017) 137 [arXiv:1612.08976] [INSPIRE].

[24] J. Drummond, J. Foster, Ö. Gürdoğan and G. Papathanasiou, *Cluster adjacency and the four-loop NMHV heptagon*, *JHEP* **03** (2019) 087 [arXiv:1812.04640] [INSPIRE].

[25] S. Caron-Huot et al., *Six-Gluon amplitudes in planar $\mathcal{N} = 4$ super-Yang-Mills theory at six and seven loops*, *JHEP* **08** (2019) 016 [arXiv:1903.10890] [INSPIRE].

[26] S. Caron-Huot et al., *The Cosmic Galois Group and Extended Steinmann Relations for Planar $\mathcal{N} = 4$ SYM Amplitudes*, *JHEP* **09** (2019) 061 [arXiv:1906.07116] [INSPIRE].

[27] L.J. Dixon and Y.-T. Liu, *Lifting Heptagon Symbols to Functions*, *JHEP* **10** (2020) 031 [arXiv:2007.12966] [INSPIRE].

[28] V. Chestnov and G. Papathanasiou, *Hexagon bootstrap in the double scaling limit*, *JHEP* **09** (2021) 007 [arXiv:2012.15855] [INSPIRE].

[29] L.J. Dixon and Y.-T. Liu, *An eight loop amplitude via antipodal duality*, *JHEP* **09** (2023) 098 [arXiv:2308.08199] [INSPIRE].

JHEP01(2025)197

[30] N. Arkani-Hamed et al., *Grassmannian Geometry of Scattering Amplitudes*, Cambridge University Press (2016) [DOI:10.1017/CBO9781316091548] [INSPIRE].

[31] S. Fomin and A. Zelevinsky, *Y systems and generalized associahedra*, hep-th/0111053 [INSPIRE].

[32] D. Gaiotto, G.W. Moore and A. Neitzke, *Wall-crossing, Hitchin systems, and the WKB approximation*, *Adv. Math.* **234** (2013) 239 [arXiv:0907.3987] [INSPIRE].

[33] B. Feng, A. Hanany, Y.-H. He and A.M. Uranga, *Toric duality as Seiberg duality and brane diamonds*, *JHEP* **12** (2001) 035 [hep-th/0109063] [INSPIRE].

[34] M. Gross, P. Hacking and S. Keel, *Birational geometry of cluster algebras*, arXiv:1309.2573.

[35] J. Drummond, J. Foster, Ö. Gürdogan and C. Kalousios, *Algebraic singularities of scattering amplitudes from tropical geometry*, *JHEP* **04** (2021) 002 [arXiv:1912.08217] [INSPIRE].

[36] N. Arkani-Hamed, T. Lam and M. Spradlin, *Non-perturbative geometries for planar $\mathcal{N} = 4$ SYM amplitudes*, *JHEP* **03** (2021) 065 [arXiv:1912.08222] [INSPIRE].

[37] N. Henke and G. Papathanasiou, *How tropical are seven- and eight-particle amplitudes?*, *JHEP* **08** (2020) 005 [arXiv:1912.08254] [INSPIRE].

[38] A. Herderschee, *Algebraic branch points at all loop orders from positive kinematics and wall crossing*, *JHEP* **07** (2021) 049 [arXiv:2102.03611] [INSPIRE].

[39] N. Henke and G. Papathanasiou, *Singularities of eight- and nine-particle amplitudes from cluster algebras and tropical geometry*, *JHEP* **10** (2021) 007 [arXiv:2106.01392] [INSPIRE].

[40] L. Ren, M. Spradlin and A. Volovich, *Symbol alphabets from tensor diagrams*, *JHEP* **12** (2021) 079 [arXiv:2106.01405] [INSPIRE].

[41] D. Chicherin, J.M. Henn and G. Papathanasiou, *Cluster algebras for Feynman integrals*, *Phys. Rev. Lett.* **126** (2021) 091603 [arXiv:2012.12285] [INSPIRE].

[42] S. He, Z. Li and Q. Yang, *Notes on cluster algebras and some all-loop Feynman integrals*, *JHEP* **06** (2021) 119 [arXiv:2103.02796] [INSPIRE].

[43] S. He, Z. Li, Y. Tang and Q. Yang, *Bootstrapping octagons in reduced kinematics from A_2 cluster algebras*, *JHEP* **10** (2021) 084 [*Erratum ibid.* **06** (2022) 079] [arXiv:2106.03709] [INSPIRE].

[44] S. He, Z. Li and Q. Yang, *Truncated cluster algebras and Feynman integrals with algebraic letters*, *JHEP* **12** (2021) 110 [*Erratum ibid.* **05** (2022) 075] [arXiv:2106.09314] [INSPIRE].

[45] S. He, Z. Li and Q. Yang, *Comments on all-loop constraints for scattering amplitudes and Feynman integrals*, *JHEP* **01** (2022) 073 [*Erratum ibid.* **05** (2022) 076] [arXiv:2108.07959] [INSPIRE].

[46] S. He, Y. Wang, Y. Zhang and P. Zhao, *Notes on Worldsheet-Like Variables for Cluster Configuration Spaces*, *SIGMA* **19** (2023) 045 [arXiv:2109.13900] [INSPIRE].

[47] S. He, Z. Li and Q. Yang, *Kinematics, cluster algebras and Feynman integrals*, arXiv:2112.11842 [INSPIRE].

[48] S. He et al., *A study of Feynman integrals with uniform transcendental weights and their symbology*, *JHEP* **10** (2022) 165 [arXiv:2206.04609] [INSPIRE].

[49] S. He, J. Liu, Y. Tang and Q. Yang, *Symbology of Feynman integrals from twistor geometries*, *Sci. China Phys. Mech. Astron.* **67** (2024) 231011 [arXiv:2207.13482] [INSPIRE].

[50] P. Zhao and Y. Wang, *Cluster alphabets from generalized worldsheets: a geometric approach to finite types*, *Phys. Rev. D* **108** (2023) 105013 [arXiv:2405.04772] [INSPIRE].

JHEP01(2025)197

[51] S. Badger, H.B. Hartanto and S. Zoia, *Two-Loop QCD Corrections to $Wb\bar{b}$ Production at Hadron Colliders*, *Phys. Rev. Lett.* **127** (2021) 012001 [arXiv:2102.02516] [INSPIRE].

[52] S. Badger, H.B. Hartanto, J. Kryś and S. Zoia, *Two-loop leading-colour QCD helicity amplitudes for Higgs boson production in association with a bottom-quark pair at the LHC*, *JHEP* **11** (2021) 012 [arXiv:2107.14733] [INSPIRE].

[53] S. Abreu et al., *Leading-color two-loop amplitudes for four partons and a W boson in QCD*, *JHEP* **04** (2022) 042 [arXiv:2110.07541] [INSPIRE].

[54] S. Badger, H.B. Hartanto, J. Kryś and S. Zoia, *Two-loop leading colour helicity amplitudes for $W^{\pm}\gamma$ + j production at the LHC*, *JHEP* **05** (2022) 035 [arXiv:2201.04075] [INSPIRE].

[55] G. Papathanasiou, *The SAGEX review on scattering amplitudes Chapter 5: analytic bootstraps for scattering amplitudes and beyond*, *J. Phys. A* **55** (2022) 443006 [arXiv:2203.13016] [INSPIRE].

[56] G. Travaglini et al., *The SAGEX review on scattering amplitudes*, *J. Phys. A* **55** (2022) 443001 [arXiv:2203.13011] [INSPIRE].

[57] T. Gehrmann, M. Jaquier, E.W.N. Glover and A. Koukoutsakis, *Two-Loop QCD Corrections to the Helicity Amplitudes for $H \to 3$ partons*, *JHEP* **02** (2012) 056 [arXiv:1112.3554] [INSPIRE].

[58] C. Duhr, *Hopf algebras, coproducts and symbols: an application to Higgs boson amplitudes*, *JHEP* **08** (2012) 043 [arXiv:1203.0454] [INSPIRE].

[59] T. Gehrmann et al., *Two-loop helicity amplitudes for H+jet production to higher orders in the dimensional regulator*, *JHEP* **04** (2023) 016 [arXiv:2301.10849] [INSPIRE].

[60] J.R. Ellis, M.K. Gaillard and D.V. Nanopoulos, *A Phenomenological Profile of the Higgs Boson*, *Nucl. Phys. B* **106** (1976) 292 [INSPIRE].

[61] M.A. Shifman, A.I. Vainshtein, M.B. Voloshin and V.I. Zakharov, *Low-Energy Theorems for Higgs Boson Couplings to Photons*, *Sov. J. Nucl. Phys.* **30** (1979) 711 [INSPIRE].

[62] T. Inami, T. Kubota and Y. Okada, *Effective Gauge Theory and the Effect of Heavy Quarks in Higgs Boson Decays*, *Z. Phys. C* **18** (1983) 69 [INSPIRE].

[63] T. Gehrmann and E. Remiddi, *Two loop master integrals for $\gamma* \to 3$ jets: the planar topologies*, *Nucl. Phys. B* **601** (2001) 248 [hep-ph/0008287] [INSPIRE].

[64] T. Gehrmann and E. Remiddi, *Two loop master integrals for $\gamma* \to 3$ jets: the nonplanar topologies*, *Nucl. Phys. B* **601** (2001) 287 [hep-ph/0101124] [INSPIRE].

[65] S. Di Vita, P. Mastrolia, U. Schubert and V. Yundin, *Three-loop master integrals for ladder-box diagrams with one massive leg*, *JHEP* **09** (2014) 148 [arXiv:1408.3107] [INSPIRE].

[66] E. Panzer, *Feynman integrals and hyperlogarithms*, Ph.D. thesis, Humboldt University, Berlin, Germany (2015) [arXiv:1506.07243] [INSPIRE].

[67] D.D. Canko et al., *N^3LO calculations for $2 \to 2$ processes using simplified differential equations*, *SciPost Phys. Proc.* **7** (2022) 028 [arXiv:2110.08110] [INSPIRE].

[68] D.D. Canko and N. Syrrakos, *Planar three-loop master integrals for $2 \to 2$ processes with one external massive particle*, *JHEP* **04** (2022) 134 [arXiv:2112.14275] [INSPIRE].

[69] J.M. Henn, J. Lim and W.J. Torres Bobadilla, *First look at the evaluation of three-loop non-planar Feynman diagrams for Higgs plus jet production*, *JHEP* **05** (2023) 026 [arXiv:2302.12776] [INSPIRE].

JHEP01(2025)197

[70] N. Syrrakos and D.D. Canko, *Three-loop master integrals for H+jet production at N3LO: towards the non-planar topologies*, *PoS* **RADCOR2023** (2024) 044 [arXiv:2307.08432] [INSPIRE].

[71] J. Drummond, J. Foster and Ö. Gürdoğan, *Cluster Adjacency Properties of Scattering Amplitudes in $N = 4$ Supersymmetric Yang-Mills Theory*, *Phys. Rev. Lett.* **120** (2018) 161601 [arXiv:1710.10953] [INSPIRE].

[72] J. Drummond, J. Foster and Ö. Gürdoğan, *Cluster adjacency beyond MHV*, *JHEP* **03** (2019) 086 [arXiv:1810.08149] [INSPIRE].

[73] O. Steinmann, *Über den Zusammenhang zwischen den Wightmanfunktionen und der retardierten Kommutatoren*, *Helv. Physica Acta* **33** (1960) 257.

[74] O. Steinmann, *Wightman-Funktionen und retardierten Kommutatoren. II*, *Helv. Physica Acta* **33** (1960) 347.

[75] K.E. Cahill and H.P. Stapp, *Optical theorems and Steinmann relations*, *Annals Phys.* **90** (1975) 438 [INSPIRE].

[76] S. Fomin and A. Zelevinsky, *Cluster algebras II: finite type classification*, *Invent. Math.* **154** (2003) 63 [math/0208229] [INSPIRE].

[77] A. Berenstein, S. Fomin and A. Zelevinsky, *Cluster algebras III: upper bounds and double Bruhat cells*, *Duke Math. J.* **126** (2005) 1 [math/0305434].

[78] S. Fomin and A. Zelevinsky, *Cluster algebras IV: coefficients*, *Compos. Math.* **143** (2007) 112 [math/0602259].

[79] A. Felikson, M. Shapiro and P. Tumarkin, *Cluster algebras and triangulated orbifolds*, *Adv. Math.* **231** (2012) 2953.

[80] B. Keller, *Cluster algebras and derived categories*, arXiv:1202.4161.

[81] M. Kontsevich and Y. Soibelman, *Stability structures, motivic Donaldson-Thomas invariants and cluster transformations*, arXiv:0811.2435 [INSPIRE].

[82] S. Fomin, L. Williams and A. Zelevinsky, *Introduction to Cluster Algebras. Chapters 1-3*, arXiv:1608.05735 [INSPIRE].

[83] S. Fomin, L. Williams and A. Zelevinsky, *Introduction to Cluster Algebras. Chapters 4-5*, arXiv:1707.07190.

[84] S. Abreu et al., *Two-Loop Integrals for Planar Five-Point One-Mass Processes*, *JHEP* **11** (2020) 117 [arXiv:2005.04195] [INSPIRE].

[85] L.J. Dixon, A.J. McLeod and M. Wilhelm, *A Three-Point Form Factor Through Five Loops*, *JHEP* **04** (2021) 147 [arXiv:2012.12286] [INSPIRE].

[86] V. Mitev and Y. Zhang, *SymBuild: a package for the computation of integrable symbols in scattering amplitudes*, arXiv:1809.05101 [INSPIRE].

[87] S. He, X. Jiang, J. Liu and Q. Yang, *On symbology and differential equations of Feynman integrals from Schubert analysis*, *JHEP* **12** (2023) 140 [*Erratum ibid.* **04** (2024) 063] [arXiv:2309.16441] [INSPIRE].

[88] E. Panzer, *Algorithms for the symbolic integration of hyperlogarithms with applications to Feynman integrals*, *Comput. Phys. Commun.* **188** (2015) 148 [arXiv:1403.3385] [INSPIRE].

[89] C. Fevola, S. Mizera and S. Telen, *Landau Singularities Revisited: Computational Algebraic Geometry for Feynman Integrals*, *Phys. Rev. Lett.* **132** (2024) 101601 [arXiv:2311.14669] [INSPIRE].

JHEP01(2025)197

[90] C. Fevola, S. Mizera and S. Telen, *Principal Landau determinants*, *Comput. Phys. Commun.* **303** (2024) 109278 [arXiv:2311.16219] [INSPIRE].

[91] M. Helmer, G. Papathanasiou and F. Tellander, *Landau Singularities from Whitney Stratifications*, arXiv:2402.14787 [INSPIRE].

[92] C. Dlapa, M. Helmer, G. Papathanasiou and F. Tellander, *Symbol alphabets from the Landau singular locus*, *JHEP* **10** (2023) 161 [arXiv:2304.02629] [INSPIRE].

[93] M. Heller, A. von Manteuffel and R.M. Schabinger, *Multiple polylogarithms with algebraic arguments and the two-loop EW-QCD Drell-Yan master integrals*, *Phys. Rev. D* **102** (2020) 016025 [arXiv:1907.00491] [INSPIRE].

[94] M. Heller, *Planar two-loop integrals for $\mu\mathbf{e}$ scattering in QED with finite lepton masses*, arXiv:2105.08046 [INSPIRE].

[95] X. Jiang, J. Liu, X. Xu and L.L. Yang, *Symbol letters of Feynman integrals from Gram determinants*, arXiv:2401.07632 [INSPIRE].

[96] A. Matijašić and J. Miczajka, *Effortless: efficient generation of odd letters with multiple roots as leading singularities*, to appear.

JHEP01(2025)197